J Mater Sci (2006) 41:5704–5708
DOI 10.1007/s10853-006-0069-9

LETTER

Bead structure variations during electrospinning of polystyrene

Goki Eda · Satya Shivkumar

Received: 24 February 2006 / Accepted: 24 March 2006 / Published online: 6 June 2006

Introduction

One of the attractive features of electrospinning is the capability to produce a wide range of fiber morphologies by controlling various material and process parameters. Other than the typically observed cylindrical fibers, flat, wrinkled, and porous fibers have been reported to date for different polymer-solvent systems [1, 2]. Koombhongse et al. [1] suggest that the morphology of the fiber obtained is determined by a complex interaction between fluid flow, electrical forces, and solvent evaporation. During the solidification of the jet, a thin skin of solid polymer can form on the surface, especially if a highly volatile solvent is used. This skin can subsequently collapse and lead to wrinkled and flat fibers. The formation of sub-micron pores on electrospun fibers is another interesting phenomenon, which has attracted attention [2, 3]. Reports have shown that humidity, molecular weight and solvent properties play an important role in pore formation. A recent study by Liu and Kumar [4] indicates that droplets of solution produced by electrospinning can also undergo skin formation and collapse, thereby developing interesting bead shapes and surface morphologies. A variety of bead morphologies including porous beads, microscopic ladles and cups can be produced by using different solvents. Although these results confirmed the significance of solvent evaporation rate and solution viscosity on bead morphology, the effect of molecular weight on attainable bead structures has not yet been explored. The ability to control the bead structures in terms of this fundamental parameter may be important in many industrial polymers for diverse applications including aerosols, surface coatings, membranes, chromatography standards and drug delivery systems. The purpose of this contribution is to examine the cumulative effects of polymer molecular weight and solution concentration on the bead structure in electrospun polystyrene. The structures that may be produced with dilute solutions before the emergence of stable fiber structures are explored.

G. Eda · S. Shivkumar (✉)
Department of Mechanical Engineering, Worcester Polytechnic Institute, 100 Institute Road, Worcester, MA 01609, USA
e-mail: shivkuma@wpi.edu

Experimental procedure

Linear polystyrene with various weight average molecular weights (M_w) having a polydispersity index of about 1 were obtained from Scientific Polymer Products, Ontario, NY. Appropriate amounts of the polymer were dissolved in tetrahydrofuran, THF, (Aldrich, reagent grade) to obtain solutions of the desired concentration. Depending on M_w, the solution concentrations were varied between 0.11 wt% and 41.8 wt%, as shown in Table 1. The polymer solution was aspirated into a 1 ml syringe equipped with an 18 gauge needle (inner diameter = 0.84 mm, 51 mm long). The syringe was placed horizontally on a syringe pump (EW-74900-00, Cole-Parmer), which was calibrated to achieve a flow rate of 3 ml/h. A potential of 10 kV and a tip-to-collector distance of 10 cm was used for all the experiments. The electrospinning apparatus was enclosed in a plexiglass chamber, which was vented during the process in order to control solvent evaporation. All experiments were conducted at room temperature and at a relative humidity between 20 and 30%. The electrospun polymer was sputter-coated with gold–palladium and was examined with a scanning electron microscope (JSM-840).

Table 1 Experimental conditions used in this study

M_w (g/mol)	C (wt%)
19,300	1.1–41.8
44,100	1.1–34.5
111,400	2.6–21.2
393,400	2.6–7.5
1,045,000	0.67–1.3
1,877,000	0.11–1.0

The weight average molecular weights (M_w) and the corresponding concentration (C) ranges at which experiments were conducted are also shown. The upper limit in concentration at each molecular weight generally corresponds to the onset of fiber formation

Results and discussion

Polymer chain entanglements play a vital role in determining the structure in the electrospun polymer. A bead dominant morphology is generally observed when a minimum degree of chain entanglements is not present [5, 6]. One of the approaches to predict the degree of entanglement is to define two critical concentrations C^* and C_e [6]. A polymer molecule in a solution may assume a conformation that is confined in a volume known as the hydrodynamic volume. In a dilute solution, the molecules within this volume are dispersed in the solvent without appreciable interactions. The limiting concentration for dilute solutions, C^*, corresponds to the solution concentration where the hydrodynamic volumes begin to overlap. The entanglement concentration, C_e, separates the semi-dilute unentangled and the semi-dilute entangled regimes. Above C_e, a steep increase in the zero shear viscosity is observed due to extensive chain entanglements. A rough estimate of C^* and C_e is given by [7–9].

$$C^* \approx \frac{1}{[\eta]} \tag{1}$$

$$C_e \approx \frac{\rho M_e^0}{M} \tag{2}$$

where $[\eta]$ is the intrinsic viscosity, M the molecular mass, ρ the polymer density, and M_e^0 the average molecular mass between entanglements in the undiluted polymer. For the Polystyrene-THF system, it has been shown that chain entanglements become significant when the product of $MC_e \sim 3 \times 10^4$ [10]. The concentrations at which fibers begin to appear along with beads are shown in Table 1. These values are generally close to the entanglement concentration, C_e. Hence, during electrospinning, stable fibrous structures may typically be observed at $C > C_e$. When $C^* < C < C_e$, a bead dominant morphology may be obtained. As can be expected from Eqs. (1) and (2), the transition from bead to fiber occurs at higher concentrations as the molecular weight is decreased. Typically, the transition from bead to bead-free fibers occurs gradually over a range of concentrations [11]. Megelski et al. [2] observed the morphological changes during electrospinning of polystyrene with THF as the solvent. Their results indicate that a bead dominant morphology (with a small fraction of emerging fibers) can be obtained at a concentration of 18 wt%. This concentration corresponds to $\frac{C}{C_e} \sim 2$, where C_e is calculated to be on the order of 10 wt% (based on Eq. (2), with $\rho = 1.05$ g/cm^3 and $M_e^0 = 18{,}100$ g/mol [8]). Similar results were obtained in the present investigation, where a bead dominant structure (with emerging fibers) was obtained for $C \sim C_e$. In this case, the beads were highly wrinkled for all molecular weights. Typical examples of wrinkled beads are shown in Fig. 1. The average size of the wrinkled beads increased with molecular weight and concentration and ranged from about 10 μm to 50 μm. Large wrinkled beads with smooth surface and almost spherical shapes (Fig. 1(a)) were generally obtained at low molecular weight ($M_w \leq 44{,}100$ g/mol) solutions at relatively high concentrations (20–30 wt%). The overall shape and the nature of wrinkles within the beads suggest that a polymer skin may have formed in the early stage of jet disintegration. Localized collapse of this skin may lead to the wrinkled surface shown in Figs. 1(a) and (b). If the skin that forms on the surface develops sufficient strength, it may resist collapse and a hollow bead may be obtained upon solvent evaporation as shown in Fig. 1(c). The wrinkled beads may also contain numerous surface pores (Fig. 1(b)). The average pore size was on the order of 200 nm, similar to the data of Casper et al. [3] and Megelski et al. [2]. Casper et al. [3] have indicated that pore formation during electrospinning is quite complex and may entail a sequence of events involving phase separation. Further, humidity may play a vital role in pore formation and M_w and polydispersity of the polymer may control the resulting pore diameters.

As the concentration is lowered below C_e, a change in bead morphology may be observed depending on M_w. The wrinkled beads may change to dimpled beads and eventually to cups as the concentration is lowered for $M_w = 111{,}400$ and 393,400 g/mol. Figure 2(a) and (b) show such a transition from dimpled beads to cups observed as the concentration is changed from 16.8 wt% to 11.8 wt%. The shape of the cups was not uniform and shallow cups and dimpled beads were observed in the same sample. Similar results have been reported by Lee et al. [12], who produced cups with polystyrene at $M_w = 140{,}000$ g/mol using THF and a concentration of 13 wt%. These results suggest that there may be a range of molecular weights and concentrations in which cups can be produced. Large cups with a porous surface were also observed (Fig. 2(c)). The size of the pores was larger on the inner side of the

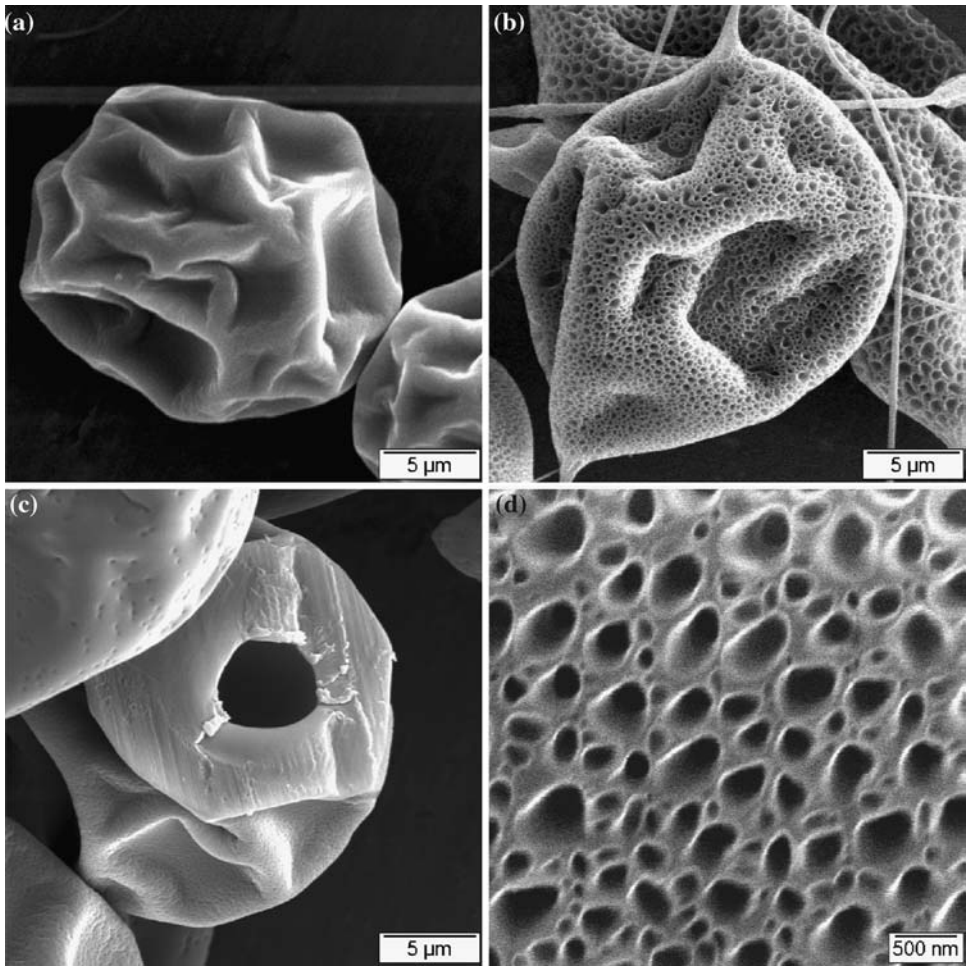

Fig. 1 Photographs showing solid (**a**) and porous (**b**) wrinkled beads. The solid beads have been sliced to reveal a hollow structure inside (**c**). A high magnification photograph of the surface pore structure in porous beads (**b**) is shown in (**d**). (**a**) and (**c**): M_w = 19,300 g/mol, C = 32.4 wt% (**b**) and (**d**): M_w = 393,400 g/mol, C = 13.9 wt%.)

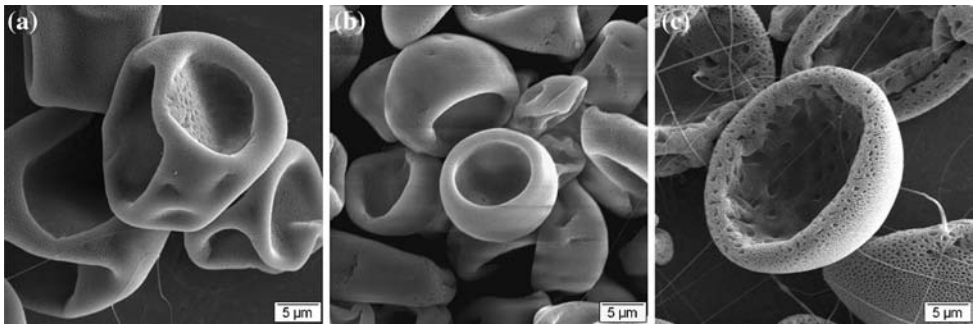

Fig. 2 Photographs showing (**a**) dimpled beads, (**b**) non-porous cups and (**c**) porous cups. (**a**) M_w = 111,400 g/mol and C = 13.9 wt%, (**b**) M_w = 111,400 g/mol, C = 11.8 wt%, and (**c**) M_w = 393,400 g/mol, C = 11.9 wt%

cup, suggesting that the pore size may depend on the stresses that are caused during the collapse of the bead.

The depth of the cup decreased gradually as the concentration was lowered further, resulting in flat dish-shaped beads (Fig. 3). The decrease in the cup depth upon dilution is consistent with the results reported by Liu and Kumar [4]. Polystyrene dishes were observed at concentrations ranging from 1 wt% to 8 wt% and M_w between 19,300 and 393,400 g/mol. Higher concentration and molecular weight typically resulted in thicker and larger dishes (Fig. 3). In this concentration regime, toroidal beads were also observed as shown in Fig. 4. The toroidal beads were typically observed with low to moderate molecular weight solutions (19,300, 44,100, and 111,400 g/mol) and were obtained together with dish-shaped beads. Polystyrene dishes typically had rims suggesting that upon collapsing of the drop, the solutions were pushed away to the edge of the beads. As can be seen from Fig. 4(b), it is likely that the holes in the toroids were formed by the radial stress caused by the solvent evaporation from the rim.

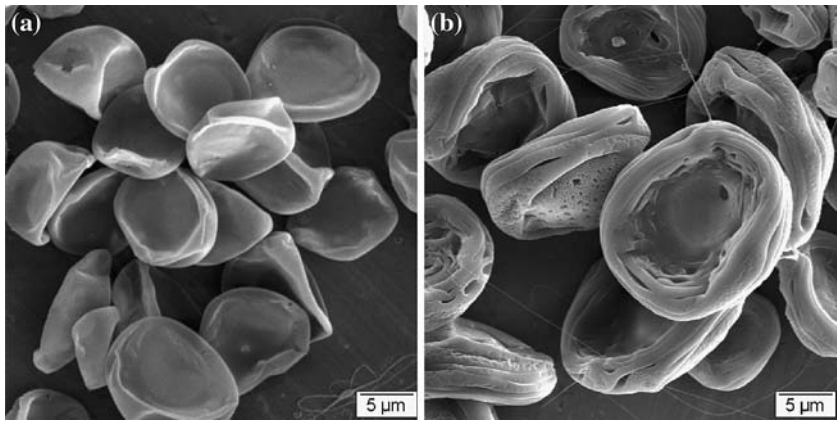

Fig. 3 Photographs showing dish-shaped beads obtained with (**a**) M_w = 19,300 g/mol, C = 1.1 wt% and (**b**) $M_{w\,=}$ 393,400, C = 3.3 wt%. It can be noted that the dish-shaped beads in (**b**) have a greater wall thickness than in (**a**)

Various morphologies such as micro-porous beads, shells, dishes and hollow porous beads can be obtained depending on M_w, as the solution concentration is adjusted to be near C^* (Fig. 5). At low molecular weight (M_w = 19,300 g/mol), the structure consisted predominantly of dishes as shown in Fig. 3(a). In this case, the concentration (1.1 wt%) was slightly below C^*. As M_w is increased to 44,100 g/mol, hollow shells with a smooth surface were obtained at C = 2.6 wt%, just below C^* (Fig. 5(a)). Some beads may collapse to dishes, but many retained nearly spherical shapes. It is likely that after the formation of a thin layer of skin, the atmospheric pressure caused the tears and the holes on the surface thereby creating channels through which the rest of the solvent escaped. Micro-porous beads were produced for M_w = 393,400 g/mol as shown in Fig. 5(b) for C = 2.6 wt% (slightly greater than C^*). The extent of porosity in the micro-porous beads increased as the concentration in this regime was lowered. An extreme example of the structure at low concentration is shown in Fig. 5(c). In this case, hollow porous beads were produced for C = 0.11 wt% (M_w = 1,877,000 g/mol).

The cumulative effects of molecular weight and concentration on the bead structure are summarized in Fig. 6. Various regions corresponding to different bead morphologies are highlighted. Related works by Megelski et al. [2] and Lee et al. [12] are also indicated. In addition, the dilute solution limit, C^* (calculated from Eq. (1) [13]), and the entanglement concentration, C_e (based on the results of Jamieson and Telford [10]), are also shown. In most cases, the transition from one type of bead to the next was gradual and neighboring structures were also observed in the same sample. A general trend in all molecular weight solutions was that upon dilution from a concentration near C_e to below C^*, the morphology of the wrinkles changed into the various structures introduced in this paper. Further investigation is critical in highlighting the mechanism of formation of these beads.

Conclusions

Various bead morphologies including wrinkled beads, cups, dishes, toroids and hollow beads can be produced by controlling the molecular weight and concentration. The surface of the beads can also contain pores on the order of 200 nm. Typically, these bead structures can be obtained from dilute and semi-dilute solutions. Wrinkled

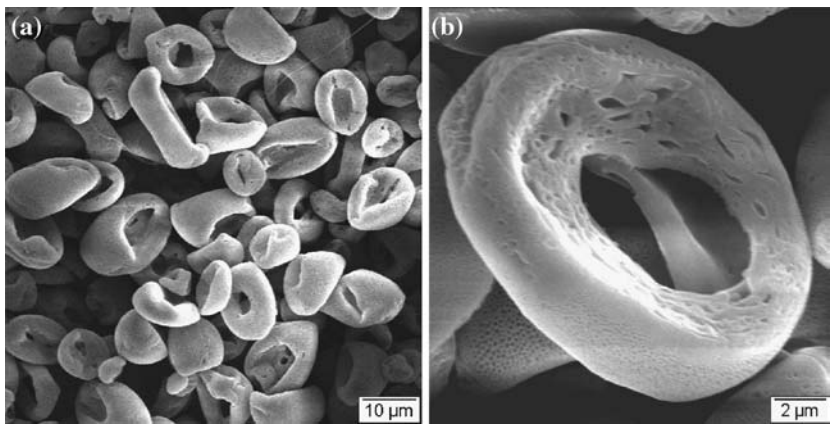

Fig. 4 Photographs (**a**) showing the toroidal beads observed at M_w = 111,400 g/mol and C = 6.3 wt%. A high magnification photograph of a single toroidal bead is shown in (**b**)

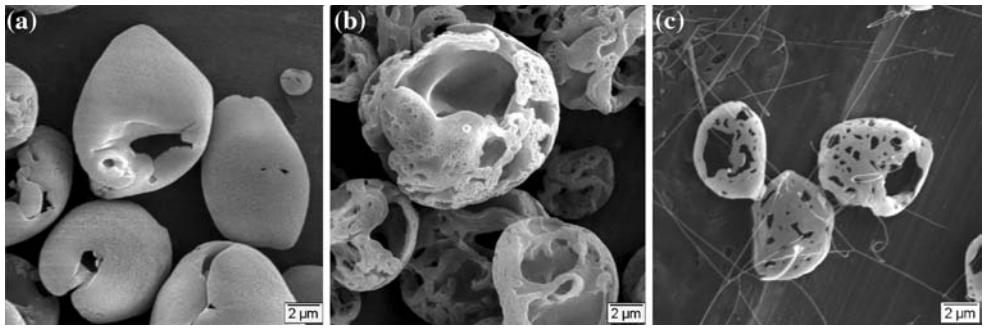

Fig. 5 Photographs showing (**a**) hollow shells (M_w = 44,100 g/mol, C = 2.6 wt%), (**b**) micro-porous beads (M_w = 393,400 g/mol, C = 2.6 wt%) and (**c**) hollow porous beads (M_w = 1,877,000 g/mol, C = 0.11 wt%)

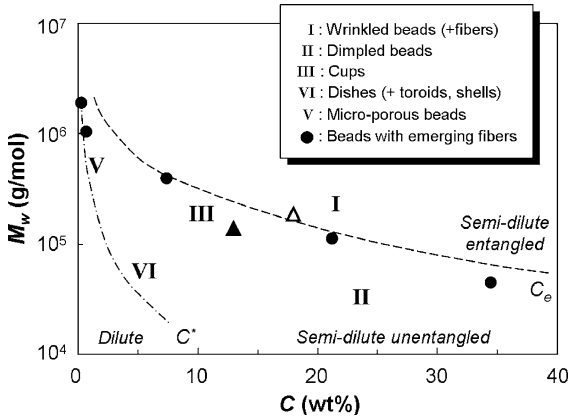

Fig. 6 Morphological variations in the bead structure as a function M_w and C showing various regimes. The structures shown in parentheses can coexist with the dominant morphology indicated. The limiting concentration at which fibers begin to appear along with beads are also shown for different molecular weights used in this study. The values for the dilute solution limit (C^*) calculated from Eq. (1) [13] and the entanglement concentration (C_e) obtained from the data of Jamieson and Telford [10] are plotted. The data of Lee et al. [12] who obtained cups (▲) and Megelski et al. [2] who obtained beads with emerging fibers (Δ) are shown

beads were obtained from semi-dilute solutions close to the entanglement concentration, C_e, for all molecular weights. As the concentration was lowered below C_e, other bead morphologies described above were obtained. Micro-porous beads and hollow skeletons were obtained for molecular weights greater than 111,400 g/mol when the concentration was near C^*, the dilute solution limit.

References

1. Koombhongse S, Liu W, Reneker DH (2001) J Polym Sci Part B 39:2598
2. Megelski S, Stephens JS, Rabolt JF, Bruce Chase D (2002) Macromolecules 35:8456
3. Casper CL, Stephens JS, Tassi NG, Chase DB, Rabolt JF (2004) Macromolecules 37:573
4. Liu J, Kumar S (2005) Polymer 46:3211
5. Shenoy SL, Bates WD, Frisch HL, Wnek GE (2005) Polymer 46:3372
6. Gupta P, Elkins C, Long TE, Wilkes GL (2005) Polymer 46:4799
7. Graessley WW (2004) Polymeric liquids and networks: structure and properties. Garland Science, New York
8. Ferry JD (1980) Viscoelastic properties of polymers, 3rd edn. Wiley, New York
9. Meerwall EDV, Amis EJ, Ferry JD (1985) Macromolecules 18:260
10. Jamieson AM, Telford D (1982) Macromolecules 15:1329
11. Zong X, Kim K, Fang D, Ran S, Hsiao BS, Chu B (2002) Polymer 43:4403
12. Lee KH, Kim HY, Bang HJ, Jung YH, Lee SG (2003) Polymer 44:4029
13. Brandrup J, Immergut EH, Grulke EA (1999) Polymer handbook, 4th edn. Wiley, New York